IEEE Access
Multidisciplinary ⋮ Rapid Review ⋮ Open Access Journal

Received 22 May 2024, accepted 25 June 2024, date of publication 1 July 2024, date of current version 10 July 2024.

Digital Object Identifier 10.1109/ACCESS.2024.3420935

RESEARCH ARTICLE

Study on the Vibration Behaviour of Locomotives Under Wheel Polygon Excitation and Its Quantitative Detection Method

WEIWEI GAN[1,2], ZHONGHAO BAI[1], QINGLIN XIE[3], (Graduate Student Member, IEEE), BINGGUANG WEN[3], XINYU QIAN[3], ZHIGANG HU[3], GONGQUAN TAO[3], ZEFENG WEN[3], AND KAN LIU[1], (Senior Member, IEEE)

[1]College of Mechanical and Vehicle Engineering, Hunan University, Changsha 410082, China
[2]Zhuzhou CRRC Times Electric Company Ltd., Zhuzhou 412001, China
[3]State Key Laboratory of Rail Transit Vehicle System, Southwest Jiaotong University, Chengdu 610031, China

Corresponding author: Qinglin Xie (qlxie@my.swjtu.edu.cn)

This work was supported in part by the National Natural Science Foundation under Grant U21A20167, in part by China Postdoctoral Science Foundation under Grant 2021T140571, and in part by Sichuan Science and Technology Program under Grant 2023YFH0049.

ABSTRACT Wheel polygons can significantly impair the operational quality, service life and ride comfort of railway systems and even threaten the safety of train operations. Timely detection of wheel polygons is of great benefit in formulating a reasonable wheel maintenance strategy. First, to investigate the vibration response of the locomotive under wheel polygon excitation, a locomotive–tack coupled dynamic model is established, taking into account the flexibility of the bogie frame, wheelset, sleeper and track structure. The effects of typical wheel polygons on the vibration behavior of the locomotive under different conditions were studied. Then, the simulation results were used to quantitatively analyze the correlation between the axle box acceleration (ABA) of the locomotive and the wheel–rail system P2 mode, the inherent modal of the wheelset, the vehicle speed, the order and the amplitude of the wheel polygons. Besides, a dataset with multiple working conditions was created from the simulation data and a quantitative wheel polygon detection model was constructed based on the deep learning algorithm. Finally, the effectiveness of the proposed detection method was verified using the real-world data of ABA and wheel polygons. The results show that the proposed method can quickly and accurately detect the dominant features of the wheel polygon, i.e. the wavelength and the corresponding roughness information.

INDEX TERMS Axle box acceleration, locomotive vehicle, quantitative detection, rigid-flexible coupled dynamics model, wheel polygon.

I. INTRODUCTION

Wheel–rail rolling contact is essential for railway vehicles to carry out the transport function. However, the complex relationship between wheel and rail can lead to a variety of out-of-roundness (OOR) wheel defects, which have a significant impact on operational safety and ride comfort. Nielsen and Johansson [1] have systematically investigated the problem of wheel OOR. They focused on the classification of wheel OOR, the description of the main causes of OOR defects and the laws of wheel OOR deformation. Subsequently, a comprehensive analysis and summary of the wheel OOR formation mechanism, dynamic effects, development process and countermeasures were presented in a series of publications [2], [3], [4], [5]. Note that the patterns and effects of wheel polygons, one of the most typical wheel OORs, are particularly complex in modern rail transport due to increasing operating speeds, axle loads, train and track systems, and societal environmental demands [6], [7]. Consequently, the study of wheel polygons has attracted more interest worldwide and has long been a popular topic in railway engineering.

The associate editor coordinating the review of this manuscript and approving it for publication was Jesus Felez.

In recent decades, many scientists and engineers have conducted extensive research on the wheel polygon through mechanism analysis, simulation modeling, modal tests and on-site investigations. They have proposed various opinions and hypotheses from different perspectives. For example, Rode et al. [8] believed that the formation of a third-order polygonal wheel is highly related to the mechanical clamping by a three-jaw chuck. Under the force of the chuck, the wheel rim undergoes elastic deformation in the radial direction and develops a small initial non-circularity at the three contact points. This non-circularity continues to develop during operation and eventually transforms into a third-order wheel polygon. Nielsen and Johansson [1] found that the non-uniformity of the wheel material has a non-negligible influence on the formation and development of wheel OOR. Kalousek and Johnson [9], in their study of rail traffic in Vancouver, found that a significant installation error of the wheelset can easily lead to a large yaw angle when the train is travelling on a straight line, increasing the transverse creepage and creep force between the wheel and rail and aggravating the wear of the wheel polygon. Tao et al. [10] proposed that the first bending vibration of the wheelset is directly related to the root cause of subway wheel polygonization. After their extensive on-site experiments, they pointed out that the mechanism of wheel polygon formation was due to the resonant frequency of the vehicle–track system. In addition to discussing the mechanism of wheel polygon formation, the effects of wheel polygon formation on vehicle vibration and noise have also been documented in numerous publications. Using a developed test scheme, Qu et al. [11] observed that the vertical axle box acceleration (ABA) of the wheelset can rapidly increase from 100g to 400g due to wheel polygon excitation. Tao et al. [12] indicated that the vibration caused by the wheel polygon can be transmitted to the car body, resulting in abnormal vibration. Test results have shown that the largest contribution to vibration occurs in the 60-100 Hz range. Note that a polygonal wheel can also lead to significant vibration in the track components. Han et al. [13] and Chen et al. [14] conducted numerical studies to investigate the effects of wheel polygons on high-speed railway bridges and substructures. The results showed that there are significant nonlinear relationships between different degrees of wheel polygons and bridges and substructures. Fang et al. [15] employed a combined FEM-BEM acoustic model to evaluate the effects of wheel polygon on wheel–rail sound radiation. They found that the wheel noise radiation decreased by 6 dB(A) after re-profiling the polygonal wheel. The authors' research group conducted a series of field tests and theoretical analyses to study the problem of excessive noise in the dining car of a high-speed train. The results demonstrated that the severely degraded polygonal wheel plays a crucial role in the abnormal interior noise [16], [17], [18].

The above-mentioned literature shows that the wheel polygon can significantly affect railway systems, e.g. through poor ride quality, excessive noise pollution, abnormal vehicle vibrations and jeopardising operational safety and reliability. Therefore, on the one hand, it is very important to explore and understand the accurate mapping relationship between the wheel polygon and the dynamic response of railway vehicles, especially the analysis of the vibration response of the vehicle excited by the wheel polygon under different boundary conditions, because abnormal vibration often leads to fatigue fractures and failure of various components of the vehicle and track, which ultimately poses a great safety risk. Due to various limitations in conducting on-site experiments, such as enormous costs and the lack of extreme operating conditions, high-fidelity numerical simulations are often used to investigate the relationship between wheel polygons and the vibration behaviour of vehicles [21]. On the other hand, it is crucial to develop a fast and accurate method for wheel polygon detection to ensure the safe and cost-effective operation of railway trains. Existing methods for wheel polygon detection can be categorized into static and dynamic detection. Traditional static methods include measurements of wheel diameter and wheel roughness using specialized instruments [19], [20]. Although this method has a relatively high accuracy, it is time-consuming and labour-intensive. In addition, this measurement can only be performed when the train is not in operation. Fortunately, dynamic detection can overcome the above shortcomings and is the current trend in detecting wheel defects on railway vehicles. Dynamic detection can be divided into wayside detection and on-board detection. With wayside detection, continuous online monitoring is not possible, making it impossible to track the development process of wheel polygons in a timely manner. The on-board detection method can check the condition of wheels in real time, and the main data source is ABA [22]. Ding et al. [23] proposed a detection method for wheel polygons based on vertical ABA and verified the reliability and engineering adaptability of the method using simulation data. Sun et al. [24] presented a method for on-board wheel polygon detection called the angular domain simultaneous averaging technique. However, instead of directly determining the properties of the wheel polygons, this method creates indirect health indicators to represent the amplitudes and orders of the wheel polygons. Song et al. [25] quantitatively explored the ABA features caused by wheel polygons with different orders and amplitudes. However, the strategy they proposed is limited because it assumes that the vehicle is travelling at a constant speed. Given the non-stationary characteristics of the measured ABA signal, Xie et al. [26] developed a data-driven system for detecting wheel polygons using improved frequency domain integration. The effectiveness and superiority of the proposed method is demonstrated by long-term tracking of the ABA signal and wheel polygon data in one cycle of wheel re-profiling. In recent years, research in the field of fault diagnosis based on data-driven algorithms has achieved remarkable results with the continuous accumulation of large amounts of data from the

condition monitoring of in-service trains and has been gradually applied to the detection of wheel–rail damage in rail transport. Xie et al. [27] reported a method for rail corrugation detection using a one-dimensional convolutional neural network and data-driven algorithms. Both measurement data and contrastive analysis proved the availability and superiority of the proposed model, which can detect the depth characteristics of rail corrugation with a relative error of less than 15% and an average relative error of 6.75%. Moreover, they constructed a data-driven convolutional regression scheme called RCNet for on-board and quantitative detection of rail corrugation roughness, which has better fitting degree, loss level and time cost [28]. Ye et al. [29] proposed a convolutional neural network-based model for inspecting wheel OOR of high-speed trains. The performance of this detection model is evaluated using a simulated database. To summarize, data-driven algorithms represented by intelligent machine learning models are currently at a preliminary stage of research for wheel–rail damage detection. There are fewer literature reports on their application to the quantitative detection of wheel polygons.

The problem of wheel polygons has been recognized as a critical issue in railway systems that needs to be addressed, but it has not yet been well solved. Railway operators can make a more scientific strategy for wheel maintenance by accurately mapping the relationship between wheel polygons and the vibration behavior of the rolling stock. Researchers can gain a deeper understanding of wheel OOR deterioration trends and triggering mechanisms by effectively detecting the status of wheel polygons. However, accurately describing the response characteristics of vehicles with wheel polygons depends on complex and sophisticated modelling theory and technology. In addition, the use of ABA to quantitatively detect wheel polygons is a major challenge. Effectively extracting the characteristic response from the ABA signal to establish an accurate mapping between ABA and wheel polygons is particularly challenging, and there are few relevant articles and reports published for reference. Against this background, this study focuses on the locomotive as a research object and conducts a study on the vibration response of the vehicle under wheel polygon excitation. Based on the analysis of the mapping relationship between the excitation and the response, we have developed an ABA data-driven quantitative wheel polygon detection model to detect the order and roughness characteristics of wheel polygons using intelligent algorithms.

The rest of this article is organized as follows. Section II briefly summarize the basic characteristics of the wheel polygon. Section III describes the modelling process of the locomotive–track coupled dynamics model in detail, including the multi-rigid dynamics of the locomotive body, the flexibility of the locomotive frame, wheelset, sleeper and track structure, and the validation of the simulation model using on-site measurement signals. In Section IV, the numerical model established is used to calculate and analyse the vibration behaviour of the vehicle excited by the wheel polygon under different operating conditions. Section V presents a quantitative method for wheel polygon detection based on a convolutional neural network algorithm. Finally, conclusions are drawn in Section VI.

II. BASIC CHARACTERISTICS OF WHEEL POLYGON

The wheel polygon, as described in [1], is characterized as a periodic variation that manifests itself as uneven wear along the circumferential direction of the wheel. The discrete Fourier transform can be used to analyze the profile of the wheel polygon, which can be defined as a sequence of spatial harmonics with different frequencies (orders), amplitudes (roughness levels) and phases. As illustrated in Figure 1(a), two polygonal wheels of the 5th- and 20th-order are expressed in polar coordinates, where the peak-to-peak value means the amplitude of the wheel polygon. Figure 1(b) shows the 20th-order wheel polygon with slight and heavy amplitudes. The amplitude of the wheel polygon usually varies in the micrometer range and in most cases is within ten micrometers. Figure 1(c) shows two wheel polygons with the same order and amplitude but different phases. In reality, a wheel polygon is often formed by the coexistence of several harmonics. The investigation of wheel polygons with a single-order is of little importance for practical engineering [26]. Figure 1(d), (e) and (f), for example, show typical measurement results of polygonal wear of the wheels of underground railways, locomotives and high-speed trains. It can be seen that none of the measurements consist of a single-order, indicating that reliable results for wheel polygon detection can only be obtained by accurately evaluating the roughness of all dominant orders. In addition to using polar coordinates to represent wheel OOR information, scientists also typically use order-roughness coordinates to represent wheel OOR features. Generally, the ISO-3095 [30] and EN 15 313 [31] standards are employed to formulate the order-roughness coordinates and evaluate the severity of the wheel polygon. Figure 2 depicts the results of the wheel polygon measurement on a high-speed train in China. The wheel OOR information is expressed in a polar coordinate as shown in Figure 2(a), and the amplitude value can reflect the deterioration of wheel OOR. In Figure 2(b), the OOR characteristics of the test wheel are quantitatively represented by the order and roughness index, which is useful for a more intuitive consideration of the state of the wheel polygon.

III. LOCOMOTIVE–TRACK COUPLED DYNAMICS MODEL

To investigate the vibration characteristics of vehicles and tracks in the medium to high frequency range and to obtain a more accurate representation of the dynamic response of locomotive wheel–rail systems subjected to polygonal wheel excitation, a dynamic coupled model for locomotive vehicles and tracks was formulated in this study using SIMPACK and ANSYS software, as shown in Figure 3. The vehicle sub-model integrates flexible wheelsets and bogie frames, while the track sub-model considers flexible sleepers and rails. The following is a detailed overview of the modeling

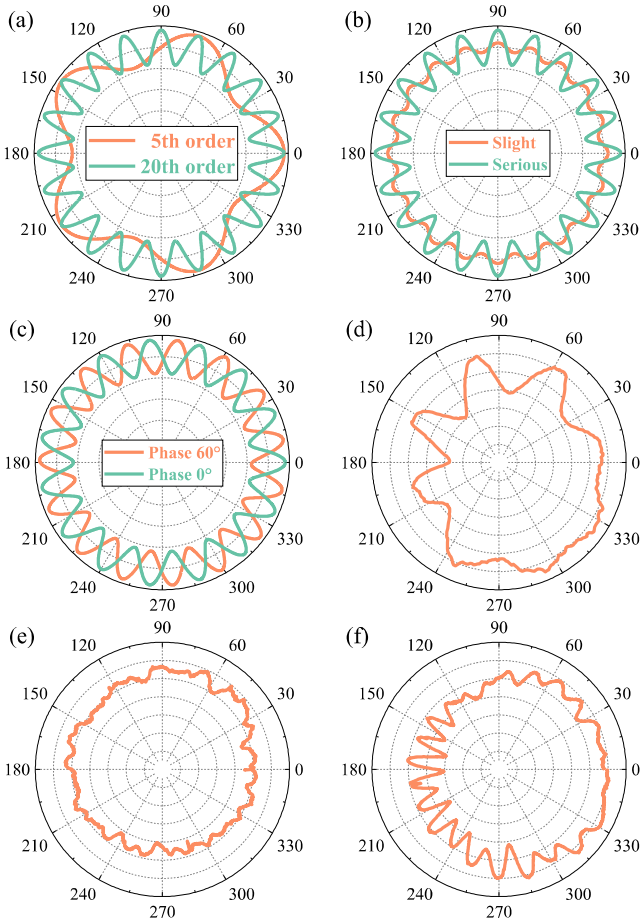

FIGURE 1. Basic features of wheel polygon with (a) different orders, (b) different amplitudes, (c) different phases, and typical measurement results of polygonal wear of (d) metro train, (e) locomotive and (f) high-speed train wheels.

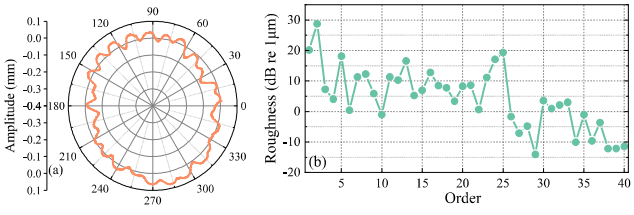

FIGURE 2. Measurement wheel polygon results in (a) polar coordinate and (b) order-roughness coordinate.

procedure, which includes multi-rigid body dynamics models for locomotive in addition to flexible wheelsets, bogie frames, and tracks.

A. MULTI-RIGID BODY DYNAMIC MODEL LOCOMOTIVES

Based on the dynamic parameters of a specific type of electric locomotive in China, a multi-rigid body dynamic model for the locomotive was established using SIMPACK software. The locomotive has a maximum operational speed of 120 km/h and consists of two identical four-axle locomotives that are coupled together. For the sake of simplicity, the

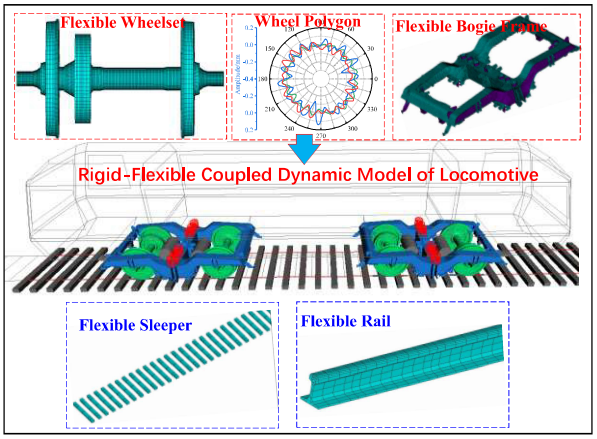

FIGURE 3. Schematic diagram of locomotive rigid-flexible coupled dynamic model.

focus of this paper is on single four-axle locomotive model, encompassing one carbody, two bogie frames, two traction rods, four motors, and four wheelsets. Specifically, the motor, adopting the nose-suspended mode, is modeled taking into account the yaw degree of freedom (DoF). The traction rod takes the pitch and yaw DoFs into account. The other rigid bodies are endowed with six DoFs each. The primary suspension system comprises axle box rods, steel springs, and vertical dampers. The second suspension system involves six high-deflection spiral steel springs, two vertical dampers, two lateral dampers, and one lateral bump stop. Symmetrically mounted lateral dampers at both ends of the bogie frame can have an anti-yaw function. Throughout the modeling process, the suspension components are modeled with spring-damping elements, which are represented by force elements in SIMPACK. The nonlinear characteristics of components such as dampers and lateral stops are fully considered. The simulation uses the locomotive profile JM3 for the wheels and the CHN60 for the rails. The normal and tangential contact issues between the wheel and rail are addressed using Hertz theory and the FastSim algorithm [32], respectively.

B. FLEXIBILITY OF WHEELSETS

The finite element analysis software ANSYS was utilized to construct the finite element model of the locomotive wheelset, employing a 6-sided solid element mesh. The material properties of the wheelset were specified with a density of 7800 kg/m^3, an elastic modulus of 210 GPa, and a Poisson ratio of 0.3. In SIMPACK, the deformation of the flexible body is calculated using the modal superposition method. To improve the simulation efficiency, it was deemed necessary to reduce the DoFs of the wheelset by selecting the main nodes in the ANSYS. The Guyan reduction method [33] was employed to obtain the reduction matrix for the wheelset substructure. Figure 4 shows the selection of main nodes for the wheelset, totaling 188 main nodes. The main nodes positioned at the nominal rolling circle of each side of the wheel, the surface of the large gear, and the axle section. All

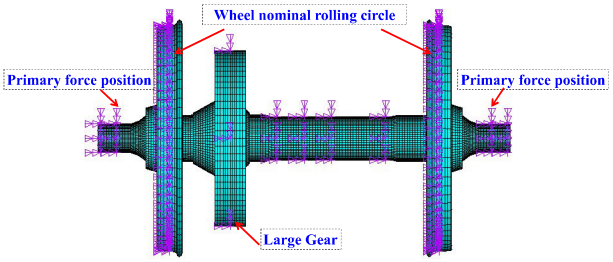

FIGURE 4. Selection of main node for wheelset.

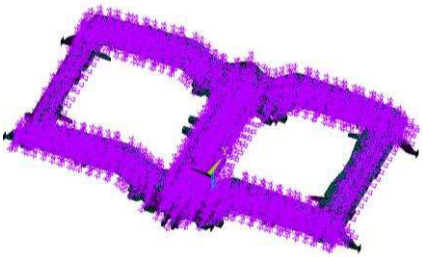

FIGURE 5. Selection of main nodes for bogie frame.

TABLE 1. Modal results for the wheelset.

Mode Descriptions	Original model	Substructure	Mode Shape
1st torsion	71.7 Hz	71.7 Hz	
1st bending	82.1 Hz	82.4 Hz	
Lateral bending of wheels	117.2 Hz	118.0 Hz	
1st umbrella shape	183.1 Hz	188.4 Hz	
Gear pitch diameter	225.9 Hz	232.0 Hz	

TABLE 2. Modal results for the bogie frame.

Mode Descriptions	Original model	Substructure	Mode Shape
1st torsion	43.2 Hz	43.2 Hz	
Vertical bending	53.6 Hz	53.6 Hz	
Lateral bending	61.6 Hz	61.7 Hz	
Diamond deformation	64.9 Hz	64.9 Hz	
2nd torsion	91.1 Hz	91.2 Hz	

main nodes account for six DoFs. To ensure the reliability of the wheelset substructure model, the Block-Lanczos method was used to calculate the modal properties of the wheelset model in its free state. The modal results of the wheelset before and after the reduction of the DoFs are shown in Table 1. A comparative analysis indicates a close resemblance in the first five modal frequencies between the original finite element model and the reduced substructure model of the wheelset. Relative to the modal impact test results of the wheelset [34], the observed relative errors in the first five modal modes are all within 2%. Therefore, the wheelset substructure model established in this study is considered accurate and reliable. During simulation, this study focuses on the first five vibration modes of the wheelset, corresponding to a cutoff frequency of 250 Hz. This range essentially encompasses the passing frequencies of polygons at different speed levels of this particular locomotive type.

C. FLEXIBILITY OF BOGIE FRAME

Due to the complexity of the bogie frame, this study first uses Hypermesh software to pre-process the 3D model of the bogie frame, including simplifying the model, meshing, etc. Then the finite element model of the bogie frame is imported into ANSYS software to select the main node for substructure analysis. The bogie frame material properties are defined with a density of 7850 kg/m^3, an elastic modulus of 210 GPa, and a Poisson ratio of 0.28. The primary structural components of the bogie frame, namely crossbeams and side beams, are modeled with shell elements, while solid elements are used for components that have similar dimensions in all three directions, such as the motor suspension seat and traction bar connection seat. Figure 5 shows the placement of 805 primary nodes evenly distributed across the surface of the bogie frame. The results of the modal analysis, both before and after the reduction of the main nodes, are shown in Table 2. In the first five modes, the modal results of the substructure model closely match those of the original finite element model. Therefore, the bogie frame substructure model established in this study is considered accurate and reliable. During the simulation process, this study accounts for modes within the initial 200 Hz range of the bogie frame.

D. FLEXIBILITY OF TRACK STRUCTURE

The flexible track structure studied in this paper consists mainly of two parts: Rails and sleepers. The rails are modeled as Timoshenko beams supported by discrete points, with a cross section of 60kg/m rails, and the meshing is done with the element Beam188. The sleeper is simplified into a parallelepiped structure, and the grid is divided by solid elements. Each sleeper has a dimension of 2.5 $\times$ 0.22$\times$ 0.16 m, a material density of 2400 kg/m^3, an elastic modulus of 32.5 GPa, and a Poisson ratio of 0.24. The sleepers are spaced at intervals of 0.58 m, with a total of 42 sleepers established. The main nodes for the rail and sleeper are chosen at intervals of 0.58 m along the track longitudinal direction. Subsequently, the flexible rail and sleeper substructure models are imported using FEMBS module of SIMPACK. Finally, the constraints for the fastenings and the foundation, which are represented by force elements, are defined in SIMPACK. The parameters pertaining to fastener and foundation forces are delineated in Table 3. During the simulation process, this study accounts for modes within the initial 200 Hz range of the sleeper.

TABLE 3. Parameters of track structure.

Parameter	values
Distance between fasteners	0.58 m
Vertical stiffness of fasteners	60 MN/m
Vertical damping of fasteners	20 kN·s/m
Vertical stiffness of foundation	120 MN/m
Vertical damping of foundation	30 N·s/m

E. MODEL VALIDATION

To ensure the reliability and precision of the locomotive vehicle track coupled dynamic model established in this paper, we analyzed the vibration acceleration of the locomotive under the excitation of the measured OOR of the wheels and compared it with the measurement results. Track irregularities are not considered during simulation, and the locomotive running speed is consistently set at 70 km/h. The sampling frequency is set at 5000 Hz. The measured polygonal excitation is applied to all eight wheels of the locomotive, as shown in Figure 6. The out-of-roundness test results of the eight wheels are presented in polar coordinates, where R and L represent the right and left wheels, respectively, and 1-4 indicate the 1st to 4th wheelsets. It can be seen that the OOR run-out values of the wheels predominantly remain within 0.2 mm, with orders primarily manifested as higher-order polygons of orders 14, 18, and 20 or higher. The relationship between the wheel polygon passing frequency, the order of the polygon, and the speed of vehicle operation is illustrated as follows:

$$f = \frac{nv}{\pi D} \tag{1}$$

where f is the passing frequency of the wheel polygon, v the vehicle speed, n the order of the wheel polygon and D the wheel diameter, with the locomotive wheel diameter specified in this study as 1.25 m. According to Eq. (1), when the locomotive operates at a speed of 70 km/h, the passing frequencies of the 14 and 18 orders are approximately 69 Hz and 89 Hz, respectively. Figure 7 compares the measured vertical acceleration data from the L2 axle box (left side of the 2nd wheelset) with simulation results. Both measured and simulated results underwent 200 Hz low-pass filtering for analysis. In Figure 7(a), it is evident that the vertical vibration acceleration magnitude from the simulation closely aligns with the measured results. The measured and simulated amplitude of vertical vibration acceleration is 69 and 63 m/s^2, respectively. while the simulated result is 63 m/s^2, indicating an 8.6% difference. Furthermore, the disparity in root mean square (RMS) values is also small, registering at 19.9 m/s^2 for the measured data and 18.5 m/s^2 for the simulated data, with a mere 7% difference between them. It can be seen that the simulation agrees with the actual vibration amplitude. The spectrum obtained by Fourier transforming the results in the time domain is shown in Figure 7(b). The analysis of the spectrum shows that the simulation model accurately reproduces the frequencies associated with the passage of the sleepers and each order of the wheel polygon. In addition, the main frequency of the vibrations calculated

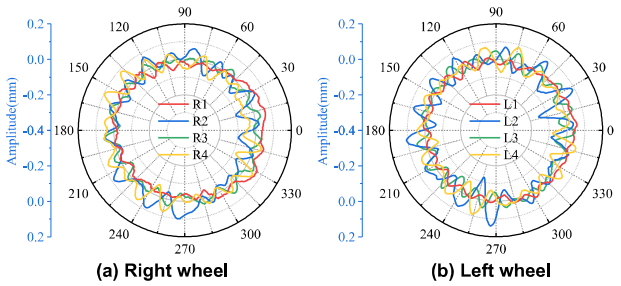

FIGURE 6. Results of measured wheel out of roundness.

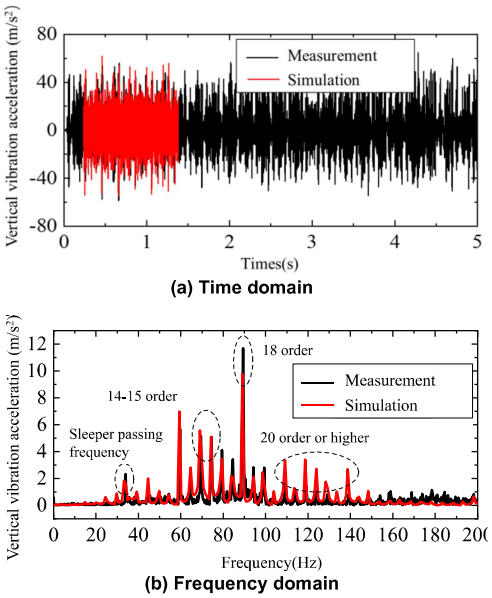

FIGURE 7. Model validation results.

by the simulations agrees well with the measured results. The main vibration frequencies are in the range of 60-90 Hz, and the highest vibration amplitude is observed at 90 Hz, which corresponds to the passage frequency of the 18th order polygon. Based on the above analysis, it becomes apparent that the locomotive–track coupled dynamic model proposed in this study can accurately reproduce the vibration behavior of the real locomotive. This implies that the model stands as a dependable tool for simulating and calculating the vehicle vibration response under wheel polygon excitation.

IV. ANALYSIS OF LOCOMOTIVE VIBRATION RESPONSE UNDER WHEEL POLYGON EXCITATION

A. ANALYSIS OF LOCOMOTIVE VIBRATION RESPONSE UNDER IDEAL HARMONIC WHEEL POLYGONS

According to the dynamic model for the coupling of locomotive and track described in Section III, a harmonic wheel polygon excitation is used in this section to investigate how variations in the wave depth and order of the wheel polygons affect the vertical vibration acceleration of the axle box. The simulation parameters are configured as follows: the polygon order ranges from 2 to 26 with a step interval of 2, and the

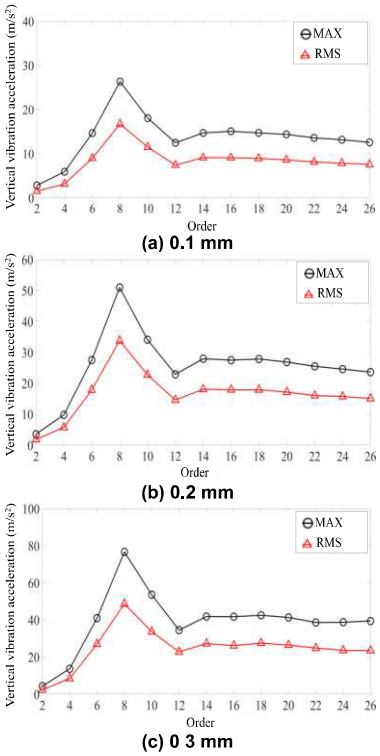

FIGURE 8. The variation of vertical ABA with the wheel polygon.

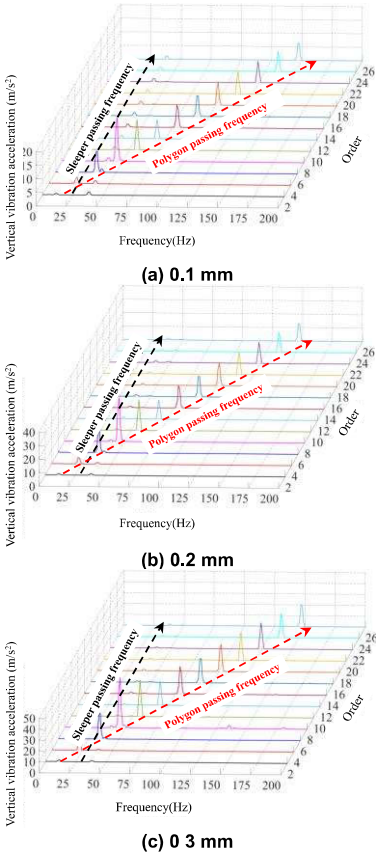

FIGURE 9. Frequency spectrum of ABA under different wheel polygons.

polygon wave depth is set at three different levels: 0.1 mm, 0.2 mm, and 0.3 mm, respectively. The wave depth is defined as the peak-to-peak value of the sine wave. The simulation is carried out at a speed of 80 km/h on a straight track without any track irregularities excitation. The polygonal excitation was applied to all wheels. Figure 8 shows the fluctuations in the maximum and RMS values of the vertical vibration acceleration of the axle box as a function of the order of the polygon. It is noteworthy that there is no direct linear relationship between the magnitude of the vibration acceleration of the axle box and the polygon order of the wheels. As the polygon order increases, both the maximum and the RMS values of the vibration acceleration of the axle box initially increase. This trend reaches its peak when the wheels experience 8th order harmonic wear. In the polygon wear case mentioned above, the passing frequency of the polygon at 45 Hz corresponds exactly to the P2 force resonance frequency of the wheel–rail system specific to this type of locomotive, which is around 42 Hz, triggering a resonance in the wheel–rail system, leading to a subsequent increase in both the maximum and RMS values of the ABA. When the polygonal order reaches or exceeds the 12th order, the changes in both the maximum and RMS values of the ABA are relatively small. When comparing the results for wave depths from 0.1 to 0.3 mm, it becomes clear that for a constant wheel polygon order, the maximum and RMS values of ABA increase with increasing polygonal wave depth. This observation underlines a direct correlation between the wave depth of the polygon and the ABA.

Figure 9 displays the frequency domain results of the vertical ABA stimulated by 2nd to 26th order wheel polygons with wave depths of 0.1 to 0.3 mm. It can be seen that each polygon order shows a small peak at 38 Hz, which corresponds to the sleeper passing frequency. The main vibration frequency matches the passing frequency of the wheel polygons, increasing with higher orders. The peaks in the frequency domain follow a similar pattern to those shown in Figure 8.

B. ANALYSIS OF LOCOMOTIVE VIBRATION RESPONSE UNDER TYPICAL MEASURED WHEEL POLYGONS

In this section, field-measured irregular polygonal wear data of locomotive wheels are used to analyze the ABA under the influence of such measured polygonal wheels. Two types of measured wheel polygon results were selected and plotted in polar coordinates and order diagrams, respectively, as shown in Figure 10 (left) and (right). In the measured wheel polygon wear of A, the dominant polygon of the wheel is 12th to 20th order. In contrast, the measured wheel polygon wear of B is characterized by eccentricity as well as the occurrence of polygon wear of order 19 to 22 and order 24.

Figures 11(a) and (b) show the variation of the maximum and RMS values of ABA with velocity under the excitation of the measured polygonal wheel wear A and B, respectively.

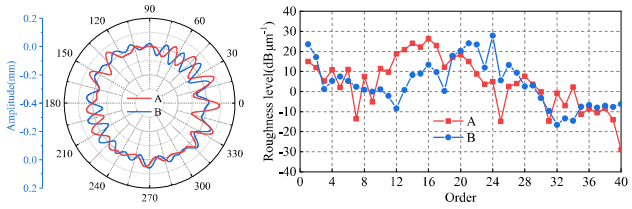

FIGURE 10. Measurement wheel polygon results in (left) polar coordinate and (right) order-roughness coordinate.

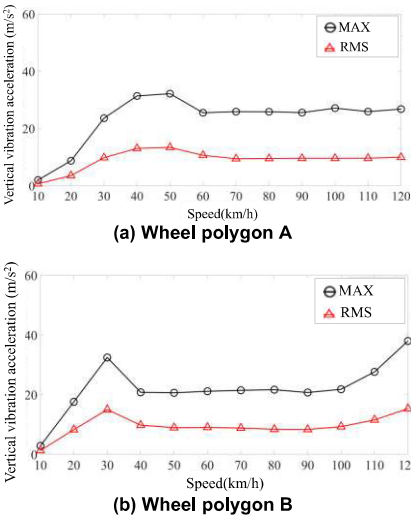

FIGURE 11. The effect of measured irregular polygon excitation on the ABA vibration under vehicle speed.

Under the excitation of the irregular polygonal wear A, both the maximum and RMS values of ABA are relatively high at a driving speed of 40 to 50 km/h. This can be attributed to the passage frequency of the 12th to 20th order polygons, which is between 33 and 58 Hz at 40 km/h and between 43 and 70 Hz at 50 km/h. At both speeds, the passage frequency of the polygons is close to the P2 frequency and thus triggers a resonance in the wheel–rail system. Similarly, under the influence of irregular polygon wear B, peaks are observed in both the maximum and RMS values of ABA when the driving speed is 30 km/h. This phenomenon has the same cause as wheel wear A, which is due to the vibrations between the wheel and rail P2. However, there is a difference: when the vehicle speed is between 110 and 120 km/h, the growth rate of both the maximum vertical ABA value and its RMS value increases significantly. This change occurs because at 120 km/h, the frequency range of polygon passes between the 19th and 24th orders falls approximately between 161 and 203 Hz. It is close to the pitch diameter of the gear (200∼225 Hz) in the wheelset constraint state. Consequently, the vertical bending of the wheelset is excited in this speed, leading to a surge in both the maximum acceleration and RMS.

Figure 12 shows the frequency domain results of ABA at various speeds. It is evident that the main vibration frequency increases with the vehicle speed. In case A, the main vibration

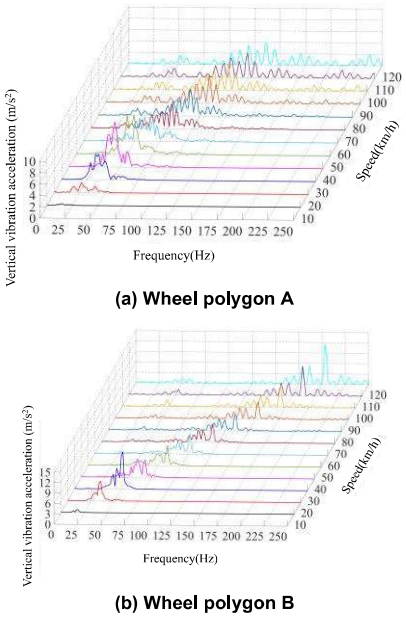

FIGURE 12. Frequency domain results of ABA under measured polygonal excitation.

frequency concentrates to 33 to 58 Hz at a speed of 40 km/h, which corresponds to the passage frequency of the 12th to 20th order polygons and is consistent with the characteristics of the measured wheel wear A. In case B, the main vibration frequency is concentrated at 55 to 70 Hz, which corresponds to the passage frequency of the 19th to 24th order polygons and is also consistent with the characteristics of the measured wheel wear. Thus, it can be concluded that under the excitation of measured irregular wheel polygons, the pattern of ABA is mainly influenced by the more prominent wheel polygon orders. When locomotive wheels exhibit polygonal wear dominated by orders 15 to 24, it is advisable to avoid traveling within the speed ranges of 30 to 50 km/h and 110 to 120 km/h.

C. ANALYSIS OF ABA RESPONSE OF LOCOMOTIVE AT DIFFERENT SPEEDS

To investigate the impact of various vehicle speeds on the ABA response of locomotive, the simulation conditions in this section are established as follows: all wheels are subjected to 18th or 24th order harmonic polygonal wear, with a fixed wave depth of 0.2 mm, and speeds ranging from 10 to 120 km/h are considered. Figure 13 depicts the correlation between vehicle speed and the maximum as well as RMS values of ABA under 18th and 24th order wheel polygons. Figure 13(a) shows an initial increase in both the maximum and RMS values of ABA as the vehicle speed increases. The peak values occur at 40 km/h and 30 km/h respectively. Beyond the 50 km/h, the changes in these values become relatively small. In Figure 13(b), a similar pattern can be observed in the variation of maximum and RMS values of ABA with vehicle speed until 100 km/h is reached. However, between

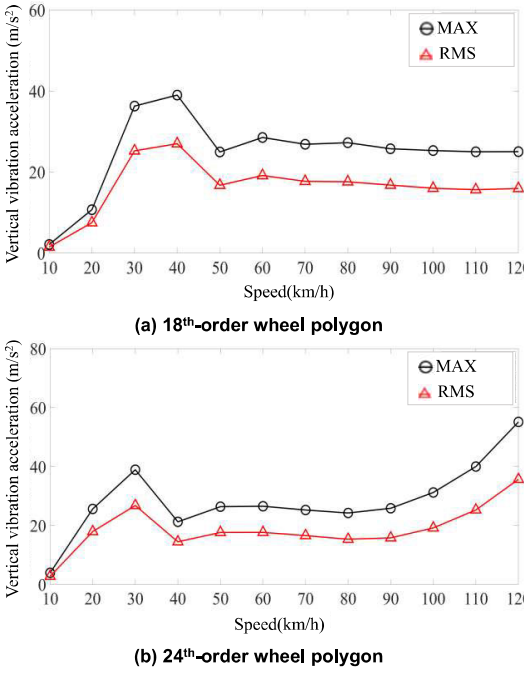

FIGURE 13. The effect of vehicle speed on the ABA under harmonic polygonal wear.

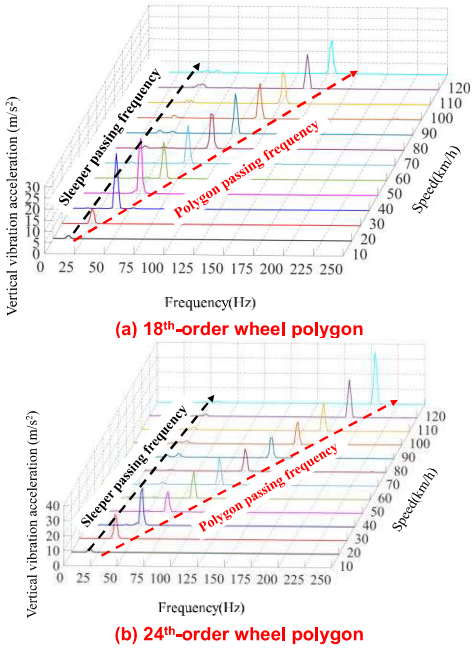

FIGURE 14. Frequency domain results of ABA.

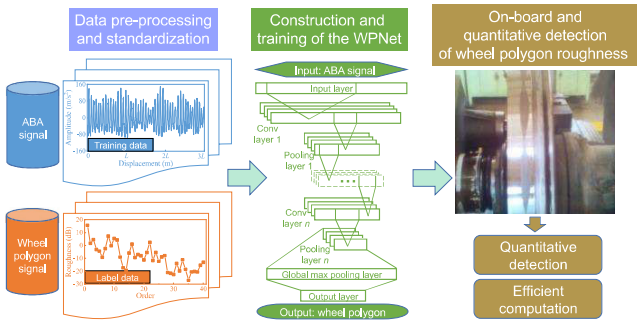

FIGURE 15. Framework of the wheel polygon roughness detection method.

100 km/h and 120 km/h, there is a secondary remarkable increase in both values. Figure 15 illustrates the frequency domain results. The trend of peak changes in the frequency domain is similar to that observed in Figure 9. These peaks is consistent with the passing frequencies of the wheel polygons at different speeds. As the speed of the vehicle increases, the passing frequency of the wheel polygon also reacts with an increase. Therefore, when formulating algorithms for detecting wheel polygons, it is crucial to consider the influence of vehicle speed on the ABA.

V. QUANTITATIVE DETECTION OF WHEEL POLYGON

From the above analysis and the relevant literatures [26], [27], [28], and [29], it is clear that wheel polygons exhibit wave-shaped harmonic wear similar to that of rail corrugation, and that the excitations they generate on the ABA are very similar. Therefore, the rail corrugation detection model developed in our previous work [28] can be adapted to enable quantitative detection of wheel polygons. This adaptation is called the wheel polygon detection network (WPNet). Figure 15 depicts the framework of the wheel polygon roughness detection method. First, the ABA and wheel polygon roughness signals are uniformly normalized to the spatial coordinate. The correlation is then further analyzed to generate corresponding training and labelling data. Second, a detection model is developed to extract ABA signal features and predict the wheel polygon roughness features. Third, the severity of wheel polygon roughness is quantitatively identified using the modified model, with the ABA signal as input.

Furthermore, it should be noted that a dynamic model with rigid-flexible coupling is used in this study to analyze the ABA under wheel polygon excitation. The execution of a single simulation case takes about 2 hours on a computer with a CPU frequency of 3.6 GHz.

A. DATA PRE-PROCESSING AND STANDARDIZATION

Data is the basis for data-driven fault diagnosis, condition monitoring and damage detection studies [35]. In order to improve the availability of the raw ABA and wheel polygon signals, targeted data pre-processing analysis is necessary. Referring to the signal processing methods in [28], the ABA response is first normalized and then converted from the time-domain to the spatial-domain. Because the speed of railway vehicles usually varies during operation. The raw ABA time-domain signal has a typical time-shift characteristic, which is not conducive to its feature extraction, and brings a challenge to the accurate detection of wheel polygon.

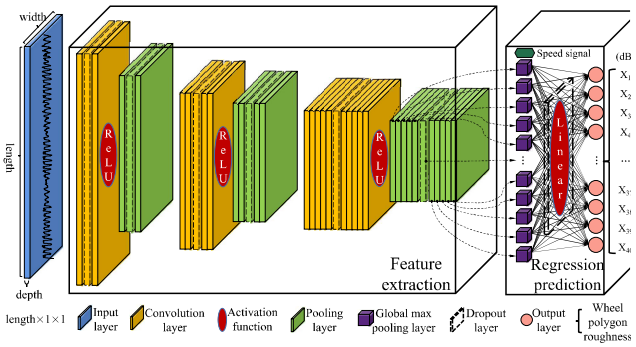

FIGURE 16. Architecture of the developed WPNet.

Hence, measurement data are uniformly converted from the time-domain to the spatial-domain to avoid the effect of vehicle speed and intuitively analyze and extract signal features. Xie et al. [26] have shown through stationarity and similarity tests that the influence of random interference in the detection of wheel defects can be reduced by analyzing the signals of 3∼6 rotation cycles of the wheel. In this study, this conclusion is taken up and the ABA signal corresponding to three wheel rotation cycles is taken as a sample. The sliced ABA signal is used as training data, while the roughness of the wheel polygon is used as label data, as it is commonly used to quantitatively characterize the severity of the wheel polygon.

B. CONSTRUCTION AND TRAINING OF THE WPNET

The WPNet is a quantitative analysis model for the detection of wheel polygon roughness. It was developed and modified on the basis of one-dimensional convolutional neural networks. The WPNet is crucial for the efficient and accurate detection of wheel polygons. Figure 16 illustrates the architecture of the WPNet, which is very similar to the model developed by Xie et al. [28] for recognizing corrugations on rails (RCNet). More details about the RCNet can be found in [28]. It is worth noting that WPNet incorporates speed information to improve the accuracy of quantitative detection of wheel polygons. Moreover, this study only focuses on the roughness of the first 40-order wheel polygons to consider their statistical properties in practice [36]. Table 4 provides the parameter settings for the WPNet. The ABA signal from three wheel rotation cycles is interpolated into a sequence with a scale of 5000 × 1 as the input signal. The output signal is a 40 × 1 vector that corresponds to the roughness properties of the first 40-order wheel polygon. During the training process, the mean squared error (MSE) is used as the loss function to guide the optimization of the WPNet model. The R-squared coefficient (R2) is used to evaluate the fitting degree between the actual values and the regression values predicted by the WPNet. As the MSE converges to zero and the R2 value approaches one, the error level decreases and the fitting degree increases, leading to more accurate wheel polygon roughness detection results.

TABLE 4. Structure and parameters setting of the WPNet.

No.	Structure	Parameters	No.	Structure	Parameters
1	Input layer	5000×1	2	Convolution layer	16×64×1
3	ReLU layer	-	4	Pooling layer	2
5	Convolution layer	32×16×1	6	ReLU layer	-
7	Pooling layer	2	8	Convolution layer	64×16×1
9	ReLU layer	-	10	Pooling layer	2
11	Global max pooling layer	-	12	Linear layer	-
13	Dropout layer	0.5	14	Output layer	40×1
15	Early stop	100			

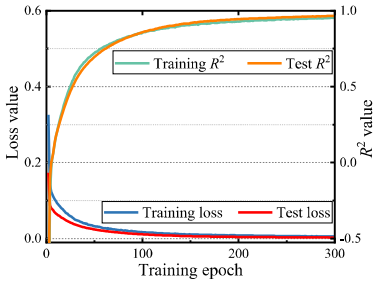

FIGURE 17. Convergence curve of loss and R2 value of WPNet model during training and testing process.

C. ON-BOARD AND QUANTITATIVE DETECTION OF WHEEL POLYGON

The dynamic model constructed in Section III can be used to determine ABA responses at different vehicle speeds and wheel polygon excitations. The wheel polygon-ABA pairs can be used as the dataset to verify the availability of the WPNet. By analyzing the simulation data based on the above-mentioned signal pre-processing method, a total of 4368 samples can be obtained, of which 80% (3494) are used as the training set for WPNet training. The remaining 20% (874) are used as the test set to evaluate the accuracy and timeliness of the WPNet. Figure 17 shows the convergence curves of the MSE and R2 values during WPNet training and testing. It can be seen that the loss level gradually converges to zero, while the R2 value increasingly approaches one as the loss decreases. Figure 18 presents two typical detection results. Figure 18(a) shows the situation where a single-order wheel polygon is prominent. It can be seen that the detection results are very close to the real values, especially for the roughness characteristic corresponding to the dominant order. Interestingly, the WPNet can maintain high accuracy in detecting the roughness feature corresponding to the dominant order when dealing with multi-order wheel polygons, as shown in Figure 18(b). Results based on simulation data show that the WPNet can quantitatively detect the wheel polygon and evaluate the roughness level.

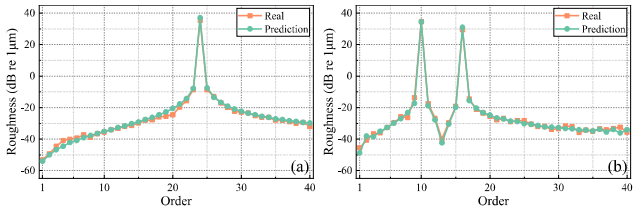

FIGURE 18. Quantitative detection results of wheel polygon roughness based on simulation data: (a) The simulation case with a 24th single-order wheel polygon and and an amplitude of 0.1 mm; (b) The simulation case with 10th and 16th multi-order wheel polygons, and corresponding amplitudes are 0.075 mm and 0.05 mm, respectively.

FIGURE 19. Measurement of (a) wheel polygons and (b) ABA using the MÜLLER-BBM device and accelerometer, respectively [36].

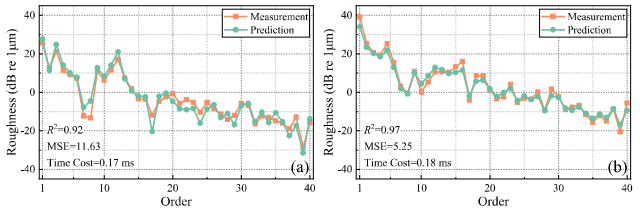

FIGURE 20. Quantitative detection results of wheel polygon roughness based on measurement data:(a) $R^2 = 0.92$; (b) $R^2 = 0.97$.

In addition to the simulation data, on-site tests were also carried out to analyze the properties of the wheel polygons and ABA of the electric locomotive. Figure 19 shows the test details of the wheel polygons and ABA. Further information about the experiment can be found in [36]. The measured wheel polygons and ABA signals were compiled into a dataset of 2778 samples according to the rule described in Section V. Based on the verified structure and the parameter settings of the WPNet, the hyper-parameters of the network are retrained using the measured dataset. The construction of the training and test set matches the simulation dataset. Figure 20 shows the detection results of the wheel polygon roughness and its measured value. It can be seen that the trend of the measurement and prediction curves are almost the same and the fitting degree is high, the error level is small and the time cost is low. This proves that the proposed WPNet maintains its efficiency even with real-world data. It can quantitatively detect the features of the wheel polygon.

VI. CONCLUSION

In this study, a locomotive–tack coupled dynamic model that takes into account the flexibility of the bogie frame, wheelset, sleeper and track structure is established to investigate the vibration behavior of the locomotive under wheel polygon excitation. The effects of wheel polygons on the locomotive ABA under different conditions were studied. Based on the simulation data, a data-driven detection method was developed to quantitatively detect wheel polygons in a timely and accurate manner. Some summaries can be concluded as follows:

(1) The maximum value and the RMS index of the locomotive ABA are in a non-linear relationship with the order of the wheel polygons and have an approximately linear correlation with the vehicle speed and the level of deterioration, i.e. the degree of roughness of the wheel polygon.

(2) When the passing frequency of the wheel polygons is close to the wheel–rail P2 resonant frequency or the natural mode frequency of the wheelset, the resonance of the wheel–rail system can be triggered and the maximum value and RMS index of the ABA increase significantly.

(3) The proposed WPNet can quantitatively detect the severity of wheel polygon roughness in combination with ABA and speed information. Both the simulation data and real-world measurement data are used to verify the availability of the WPNet. The results show that the quantitative fitting degree of wheel polygon roughness is high (over 0.9), the error level is small and the time cost is low (about 0.20 ms).

REFERENCES

[1] J. C. O. Nielsen and A. Johansson, "Out-of-round railway wheels—A literature survey," *Proc. Inst. Mech. Eng., F, J. Rail Rapid Transit*, vol. 214, no. 2, pp. 79–91, 2000.

[2] J. C. O. Nielsen, R. Lundén, A. Johansson, and T. Vernersson, "Train-track interaction and mechanisms of irregular wear on wheel and rail surfaces," *Vehicle Syst. Dyn.*, vol. 40, nos. 1–3, pp. 3–54, 2010.

[3] D. W. Barke and W. K. Chiu, "A review of the effects of out-of-round wheels on track and vehicle components," *Proc. Inst. Mech. Eng., F, J. Rail Rapid Transit*, vol. 219, no. 3, pp. 151–175, 2005.

[4] P. Wang, G. Tao, X. Yang, C. Xie, W. Li, and Z. Wen, "Analysis of polygonal wear characteristics of Chinese high-speed train wheels," *J. Southwest Jiaotong Univ.*, vol. 58, no. 6, 1357–1365, 2023.

[5] G. Tao, Z. Wen, X. Jin, and X. Yang, "Polygonisation of railway wheels: A critical review," *Railway Eng. Sci.*, vol. 28, no. 4, pp. 317–345, Dec. 2020.

[6] J. C. O. Nielsen, A. Mirza, S. Cervello, P. Huber, R. Müller, B. Nelain, and P. Ruest, "Reducing train-induced ground-borne vibration by vehicle design and maintenance," *Int. J. Rail Transp.*, vol. 3, no. 1, pp. 17–39, Jan. 2015.

[7] S. Ouakka, O. Verlinden, and G. Kouroussis, "Railway ground vibration and mitigation measures: Benchmarking of best practices," *Railway Eng. Sci.*, vol. 30, no. 1, pp. 1–22, Mar. 2022.

[8] W. Rode, D. Müller, and J. Villman, "Results of DB AG investigations-out-of-round wheels," in *Proc. Corrugation Symp.-Extended Abstr.* Berlin, Germany: IFV Bahntechink, 1997.

[9] J. Kalousek and K. L. Johnson, "An investigation of short pitch wheel and rail corrugations on the Vancouver mass transit system," *Proc. Inst. Mech. Eng., F, J. Rail Rapid Transit*, vol. 206, no. 2, pp. 127–135, 1992.

[10] G. Tao, C. Xie, H. Wang, X. Yang, C. Ding, and Z. Wen, "An investigation into the mechanism of high-order polygonal wear of metro train wheels and its mitigation measures," *Vehicle Syst. Dyn.*, vol. 59, no. 10, pp. 1557–1572, Oct. 2021.

[11] S. Qu, J. Wang, D. Zhang, H. Shi, P. Wu, and H. Dai, "Field investigation on the higher-order polygon wear on wheel of high speed trains," in *Proc. 11th Int. Conf. Contact Mech. Wear Rail/Wheel Syst. (CM)*, Delft, The Netherlands, 2018, pp. 818–823.

[12] G. Tao, Z. Wen, Q. Guan, W. Lu, Q. Fu, X. Jin, and L. Wang, "Experimental investigation of the abnormal vibration of the electric locomotive," in *Proc. 18th Int. Wheelset Congr. (IWC)*, Chengdu, China, Nov. 2016, pp. 44–49.
[13] Z. Han, Z. Chen, and W. Zhai, "Effect of wheel polygonal wear on dynamic responses of high speed train-track-bridge system," in *Proc. 25th Int. Symp. Dyn. Vehicles Roads Tracks (IAVSD)*, Rockhampton, QLD, Australia, 2017, pp. 823–828.
[14] M. Chen, Y. Sun, Y. Guo, and W. Zhai, "Study on effect of wheel polygonal wear on high-speed vehicle-track-subgrade vertical interactions," *Wear*, vols. 432–433, Aug. 2019, Art. no. 102914.
[15] J. Fang, X. Xiao, L. Wu, and X. Jin, "Influence of subway LIM train wheel polygonization on the vibration and sound radiation characteristics of it," in *Proc. Noise Vib. Mitigation Rail Transp. Syst. (IWRN)*, Berlin, Germany, 2010, pp. 117–124.
[16] J. Zhang, X. Xiao, G. Han, Y. Deng, and X. Jin, "Study on abnormal interior noise of high-speed trains," in *Proc. Noise Vib. Mitigation Rail Transp. Syst. (IWRN)*, Berlin, Germany, 2013, pp. 691–698.
[17] J. Zhang, G. Han, X. Xiao, R. Wang, Y. Zhao, and X. Jin, "Influence of wheel polygonal wear on interior noise of high-speed trains," *Zhejiang Univ.-Sci. A (Appl. Phys. Eng.)*, vol. 15, no. 12, pp. 1002–1018, 2014.
[18] G. Han, J. Zhang, X. Xiao, D. Cui, and X. Jin, "Study on high-speed train abnormal interior vibration and noise related to wheel roughness," *J. Mech. Eng.*, vol. 50, no. 22, pp. 113–121, 2014.
[19] F. Zheng, B. Zhang, R. Gao, and Q. Feng, "A high-precision method for dynamically measuring train wheel diameter using three laser displacement transducers," *Sensors*, vol. 19, no. 19, p. 4148, Sep. 2019.
[20] Z.-F. Zhang, Z. Gao, Y.-Y. Liu, F.-C. Jiang, Y.-L. Yang, Y.-F. Ren, H.-J. Yang, K. Yang, and X.-D. Zhang, "Computer vision based method and system for online measurement of geometric parameters of train wheel sets," *Sensors*, vol. 12, no. 1, pp. 334–346, Dec. 2011.
[21] X. Wu, S. Rakheja, H. Wu, S. Qu, P. Wu, H. Dai, J. Zeng, and A. K. W. Ahmed, "A study of polygonal wheel wear through a field test programme," *Vehicle Syst. Dyn.*, vol. 57, no. 6, pp. 914–934, Jun. 2019.
[22] W. Cai, M. Chi, X. Wu, J. Sun, Y. Zhou, Z. Wen, and S. Liang, "A long-term tracking test of high-speed train with wheel polygonal wear," *Vehicle Syst. Dyn.*, vol. 59, no. 5, 1–24, 2020.
[23] J. Ding, L. Lin. C. Yi, Y. Yi, and C. Huang, "Dynamic detection of out-of-round wheels using a comparison of time-frequency feature locatings," *J. Vib. Shock*, vol. 32, no. 19, pp. 39–43, 2013.
[24] Q. Sun, C. Chen, A. H. Kemp, and P. Brooks, "An on-board detection framework for polygon wear of railway wheel based on vibration acceleration of axle-box," *Mech. Syst. Signal Process.*, vol. 153, no. 2, May 2021, Art. no. 107540.
[25] Y. Song, L. Liang, Y. Du, and B. Sun, "Railway polygonized wheel detection based on numerical time-frequency analysis of axle-box acceleration," *Appl. Sci.*, vol. 10, no. 5, p. 1613, Feb. 2020.
[26] Q. Xie, G. Tao, S. M. Lo, W. Cai, and Z. Wen, "High-speed railway wheel polygon detection framework using improved frequency domain integration," *Vehicle Syst. Dyn.*, vol. 62, no. 6, pp. 1424–1445, Jun. 2024.
[27] Q. Xie, G. Tao, B. He, and Z. Wen, "Rail corrugation detection using one-dimensional convolution neural network and data-driven method," *Measurement*, vol. 200, Aug. 2022, Art. no. 111624.
[28] Q. Xie, G. Tao, S. M. Lo, X. Yang, and Z. Wen, "A data-driven convolutional regression scheme for on-board and quantitative detection of rail corrugation roughness," *Wear*, vols. 524–525, Jul. 2023, Art. no. 204770.
[29] Y. Ye, B. Zhu, P. Huang, and B. Peng, "OORNet: A deep learning model for on-board condition monitoring and fault diagnosis of out-of-round wheels of high-speed trains," *Measurement*, vol. 199, Aug. 2022, Art. no. 111268.
[30] European Committee for Standardization, *BS EN ISO 3095: 2013. Acoustics—Railway Applications—Measurement of Noise Emitted by Railbound Vehicles*, British Standards Institution, London, U.K., 2013.
[31] European Committee for Standardization. *EN 15313-2010, Railway Applications—In-Service Wheelset Operation Requirements—In-Service and Off-Vehicle Wheelset Maintenance*, British Standards Institution Publications, London, U.K., 2016.
[32] J. J. Kalker, "A fast algorithm for the simplified theory of rolling contact," *Vehicle Syst. Dyn.*, vol. 11, no. 1, pp. 1–13, Feb. 1982.
[33] R. J. Guyan, "Reduction of stiffness and mass matrices," *AIAA J.*, vol. 3, no. 2, p. 380, Feb. 1965.
[34] G. Tao, "Investigation into the formation mechanism of the polygonal wear of HXD electric locomotive wheels," doctoral thesis, Southwest Jiaotong Univ., Chengdu, China, 2018.
[35] Q. Xie, G. Tao, C. Xie, and Z. Wen, "Abnormal data detection based on adaptive sliding window and weighted multiscale local outlier factor for machinery health monitoring," *IEEE Trans. Ind. Electron.*, vol. 70, no. 11, pp. 11725–11734, Nov. 2023.
[36] G. Tao, L. Wang, Z. Wen, Q. Guan, and X. Jin, "Experimental investigation into the mechanism of the polygonal wear of electric locomotive wheels," *Vehicle Syst. Dyn.*, vol. 56, no. 6, pp. 883–899, Jun. 2018.

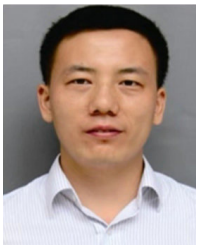

WEIWEI GAN received the M.S. degree in power electronics and power transmission from Xi'an Jiaotong University, Xi'an, China, in 2010. He is currently pursuing the Ph.D. degree with the School of Mechanical and Vehicle Engineering, Hunan University, Changsha, China.

Since 2010, he has been an Engineer with CRRC Zhuzhou Electric Locomotive Research Institute Company Ltd. He has been engaged in the research of traction control of rail transit and led the research of traction control algorithm of the fully autonomous Fuxing China Standard EMU, and the research results are now applied in batches to Fuxing China Standard EMU.

Mr. Gan's awards and honors include the 19th China Patent Gold Award, the first prize of Science and Technology of Railway Society, and the Science and Technology Progress Award of Hunan Province.

ZHONGHAO BAI received the B.S. degree in automotive engineering and the M.S. and Ph.D. degrees in vehicle engineering from Hunan University, Changsha, China, in 2000, 2002, and 2006, respectively. Since 2003, he has been with the College of Mechanical and Vehicle Engineering, Hunan University. He is currently a Full Professor and the Director of the Vehicle Safety Research Center, Hunan University. His research interests include intelligent new energy vehicles, automotive safety, automotive electronics, and automotive structural design.

QINGLIN XIE (Graduate Student Member, IEEE) received the B.S. degree in engineering mechanics and the M.S. degree in vehicle engineering from Southwest Jiaotong University, China, in 2018 and 2021, respectively, where he is currently pursuing the Ph.D. degree with the State Key Laboratory of Rail Transit Vehicle System. His research interests include intelligent operation and maintenance of wheel–rail systems, rail transit digital platform construction, and SHM data mining.

BINGGUANG WEN received the B.S. degree in mechanical manufacturing and automation from Chang'an University, in 2020, and the M.S. degree in vehicle engineering from Southwest Jiaotong University, China, in 2023, where he is currently pursuing the Ph.D. degree with the State Key Laboratory of Rail Transit Vehicle System. His research interests include simulation of wheel–rail wear evolution and vehicle dynamics performance.

XINYU QIAN received the B.S. degree in vehicle engineering from Nanjing Tech University, China, in 2021. He is currently pursuing the M.S. degree with the State Key Laboratory of Rail Transit Vehicle System, Southwest Jiaotong University. His research interests include intelligent operation and maintenance of wheel–rail systems.

ZHIGANG HU received the B.S. degree in vehicle engineering from East China Jiaotong University, China, in 2020. He is currently pursuing the M.S. degree with the State Key Laboratory of Rail Transit Vehicle System, Southwest Jiaotong University. His research interests include intelligent operation and maintenance of wheel–rail systems.

GONGQUAN TAO received the B.S. degree in engineering structure analysis and the M.S. and Ph.D. degrees in vehicle operation engineering from Southwest Jiaotong University, Chengdu, China, in 2011, 2013, and 2018, respectively. Since 2019, he has been with the State Key Laboratory of Rail Transit Vehicle System, Southwest Jiaotong University. He is currently an Associate Professor. His research interests include wheel–rail interaction, wheel and rail health management, and fault diagnosis.

ZEFENG WEN received the B.S. degree in mechanical engineering and the M.S. and Ph.D. degrees in vehicle operation engineering from Southwest Jiaotong University, Chengdu, China, in 1998, 2000, and 2006, respectively. Since 2006, he has been with the State Key Laboratory of Rail Transit Vehicle System, Southwest Jiaotong University. He is currently a Full Professor and the Deputy Director. His research interests include wheel–rail interaction and vibration and noise.

KAN LIU (Senior Member, IEEE) received the B.E. and Ph.D. degrees in automation from Hunan University, Changsha, China, in 2005 and 2011, respectively, and the Ph.D. degree in electronic and electrical engineering from The University of Sheffield, Sheffield, U.K., in 2013.

From 2013 to 2016, he was a Research Associate with the Department of Electronic and Electrical Engineering, The University of Sheffield. From 2016 to 2017, he was a Lecturer with the Control Systems Group, Loughborough University. He is currently a Professor of electromechanical engineering with Hunan University. He is also the Director of the Engineering Research Center of Ministry of Education on Automotive Electronics and Control Technology, China. His research interests include parameters estimation and sensorless control of permanent magnet synchronous machine drives, advanced design, and control solutions of high-power density converters, for applications ranging from electric locomotive and automotive, to servo motor, and drive.

Prof. Liu is now a Chief Scientist of National Key Research and Development Program and serves as an Associate Editor for IEEE Access and the *CES Transactions on Electrical Machines and Systems*.